 The removal of the sulfate anion from water using synthetic hydrotalcite (Mg/Al LDH) was investigated using powder x-ray diffraction (XRD) and thermogravimetric analysis (TG). Synthetic hydrotalcite $Mg_6Al_2(OH)_{16}(CO_3) \cdot 4H_2O$ was prepared by the co-precipitation method from aluminum and magnesium chloride salts. The synthetic hydrotalcite was thermally activated to a maximum temperature of 380°C. Samples of thermally activated hydrotalcite where then treated with aliquots of 1000ppm sulfate solution. The resulting products where dried and characterized by XRD and TG. Powder XRD revealed that hydrotalcite had been successfully prepared and that the product obtained after treatment with sulfate solution also conformed well to the reference pattern of hydrotalcite. The d(003) spacing of all samples was found to be within the acceptable region for a LDH structure. TG revealed all products

Sulfate Intercalated Layered Double Hydroxides Prepared by the Reformation Effect

Frederick L. Theiss, Sara J. Palmer, Godwin A. Ayoko, and Ray L. Frost[•]

Chemistry Discipline, Faculty of Science and Technology, Queensland University of Technology, Brisbane Queensland 4001, Australia.

Abstract

The removal of the sulfate anion from water using synthetic hydrotalcite (Mg/Al LDH) was investigated using powder x-ray diffraction (XRD) and thermogravimetric analysis (TG). Synthetic hydrotalcite $Mg_6Al_2(OH)_{16}(CO_3) \cdot 4H_2O$ was prepared by the co-precipitation method from aluminum and magnesium chloride salts. The synthetic hydrotalcite was thermally activated to a maximum temperature of 380°C. Samples of thermally activated hydrotalcite where then treated with aliquots of 1000ppm sulfate solution. The resulting products where dried and characterized by XRD and TG. Powder XRD revealed that hydrotalcite had been successfully prepared and that the product obtained after treatment with sulfate solution also conformed well to the reference pattern of hydrotalcite. The $d_{(003)}$ spacing of all samples was found to be within the acceptable region for a LDH structure. TG revealed all products underwent a similar decomposition to that of hydrotalcite. It was possible to propose a reasonable mechanism for the thermal decomposition of a sulfate containing Mg/Al LDH. The similarities in the results may indicate that the reformed hydrotalcite may contain carbonate anion as well as sulfate. Further investigation is required to confirm this.

Keywords: Sulfate, layered double hydroxide, hydrotalcite, powder x-ray diffraction, thermogravimetric analysis, water purification.

[•] Author to whom correspondence should be addressed (r.frost@qut.edu.au)

Introduction

Layered double hydroxides (LHDs) are also known as hydrotalcite like materials or anionic clays. Many LDHs such as hydrotalcire, takovite, carrboydite, reevesite, honessite, pyroaurite and iowaite occur in nature while others have been prepared synthetically in the laboratory [1-6]. LDHs are based on the brucite ($Mg(OH)_2$) structure in which some divalent layer cations are replaced with trivalent cations (Al^{3+} in the case of hydrotalcite). The result of this substitution is a layered structure carrying a net positive charge. This positive charge is balanced by anions intercalated between the layers [7, 8]. LDHs follow the general formula:

$$[M_{1-x}^{2+}M_x^{3+}(OH)_2]^{x+}[A^{n-}]_{x/n} \cdot mH_2O \tag{1}$$

Where M^{2+} and M^{3+} are the divalent and trivalent layer cations respectively, $0.2 < x < 0.33$ and A^{n-} is the exchangeable anion. [8-11]

 LDHs exhibit several unusual properties, the most interesting is known as the reformation effect. When a LDH is calcined usually at 300 - 500°C interlayer water and anions as well as the hydroxyl groups are eliminated. The result is a mixed metal oxide [12, 3, 13]. This process is also known as thermal activation. When the calcined LDH is placed in solution containing anions, the LDH structure can re-form. Whether the original structure is formed depends on a number of factors, including the nature of the lattice cations and the calcination temperature [8, 14]. In this process water is adsorbed to form the hydroxyl layers, and anions present in the solution will be adsorbed into the interlayer to balance the positive charge of the layers [12]. The reformation effect already has been used to remove a range of anions from water [15, 14, 16-19]. In this paper, we report on the removal of the sulfate anion from water under normal atmospheric conditions (not under an inert atmosphere) using synthetic hydrotalcite prepared by the co-precipitation method.

Experimental Procedure

Preparation of $Mg_6Al_2(OH)_{16}(CO_3) \cdot 4H_2O$

All reagents used in the experiments described in this paper were AR grade. Sodium hydroxide and sodium sulfate where obtained from Ajax Finechem Pty Ltd. Magnesium chloride hexahydrate and Aluminum chloride hexahydrate where obtained from Clem-Supply. Sodium

55   carbonate was obtained from MERCK Pty Limited. All chemicals where used as received with

56   no additional purification or pretreatment.

57

58   A large batch of $Mg_6Al_2(OH)_{16}(CO_3)\cdot4H_2O$ (synthetic hydrotalcite) was prepared by the co-

59   precipitation method for the use in this and other experiments. A mixed metal solution was

60   prepared by dissolving aluminum chloride hexahydrate (603.6g) and magnesium chloride

61   hexahydrate (1524.7g) in deionised water (10,000cm^3). The caustic solution was prepared by

62   slowly dissolving sodium hydroxide (800.2g) and sodium carbonate (1690.9g) in deionised

63   water (10,000cm^3). The mixed metal solution was added drop wise from a separating funnel to

64   the caustic solution while stirring. The pH of the solution was monitored using a pH probe and

65   found to average 12.2. Additional sodium hydroxide was added first in granular form then in a

66   solution to keep the pH above 10.

67

68   As soon as the two solutions where combined the hydrotalcite formed as a white precipitate.

69   The hydrotalcite was collected by vacuum filtration and washed with 0.1 M sodium carbonate

70   solution (10,000cm^3). The hydrotalcite was collected and dried in an oven at approximately

71   80°C. When the hydrotalcite was dry it was ground with a mortar and pestle and then

72   homogenized by combining all the samples into a large glass dish and thoroughly mixed. The

73   total mass of hydrotalcite obtained was 927.6g.

74   **Thermal Activation and Reformation**

75   Approximately 150g of the Mg/Al LDH was thermally activated in a furnace to a maximum

76   temperature of 380°C. The rate of heating averaged at 20°C/minute up to the set temperature,

77   and was left at that temperature for 1 hour. A 1000ppm solution was prepared by dissolving

78   sodium sulfate (2.2158g) in deionised water (500cm^3). Two amounts of sample were used in

79   this investigation, 3 and 10g. The experiment was repeated to confirm the results.

80   Each sample was then treated with a 20cm^3 aliquot of the 1000ppm sulfate solution. Each

81   sample was then stirred for 30 minutes. The mixture was separated by vacuum filtration. The

82   solids were recovered for further analysis and dried in an oven at approximately 80°C for

83   approximately two days. The filtrate was collected using a syringe filter (0.45μm) to remove

84   any remaining particulate material before further analysis.

85 **Characterization of Synthetic Hydrotalcite**

86 X-ray diffraction patterns were collected using a Philips X'pert wide angle X-Ray

87 diffractometer, with Cu Ka radiation (1.54052 Å).

88

89 Thermal analysis was carried out using a TA® Instruments incorporated high resolution

90 thermogravimetric analyser (series Q500) under a flowing nitrogen atmosphere ($40 cm^3$/min).

91 The sample (77.365mg and 63.228mg for the 1g and 10g samples respectively) was placed in

92 an open platinum pan and heated from room temperature at a rate of 2.50°C/min to a maximum

93 temperature of 1000°C. TG and DTG curves where obtained however a mass spectrometer was

94 not available for evolved gas analysis.

95

Results and Discussion

96

97 **Powder XRD**

98 The Powder XRD results shown in Fig 1 indicate that a LDH structure was successfully

99 formed. The XRD pattern closely fits that of synthetic hydrotalcite which is the Mg/Al LDH.

100 Sodium chloride was still present in the sample despite the washing process. There was also

101 some indication that small amounts of sodium carbonate hydrate may be present in the

102 precipitate. The $d_{(003)}$ spacing was found to be 7.81 Å, which was consistent with a LDH

103 structure. [14, 8]

104

105 Thermal activation caused a clear change in the XRD pattern as expected. The results are

106 presented in Fig 2. Comparison of pattern shown in Fig 1 with that of the thermally activated

107 LDH shown in Fig 2 shows the LDH structure was lost with thermal activation and regenerated

108 after treatment with sulfate solution. This observation confirms the reformation process of LDH

109 structures. Some phases that may be present in the thermally activated hydrotalcite include

110 NaCl, $Na_3Mg(CO_3)_2Cl$, AlO(OH) and $Na_2Mg(CO_3)_2$. The $d_{(003)}$ spacing was found to increase

111 to 8.13 Å. After reformation in the sodium sulfate solution, the LDH structure was successfully

112 reconstructed. Minimal change in the $d_{(003)}$ spacing was observed for the treated thermally

113 activated hydrotalcites (7.83 and 7.76 Å for the 3g and 10g samples, respectively) compared to

114 the original hydrotalcite (7.81 Å). There did not appear to be any additional phases that formed

115 after the reformation process compared to the original hydrotalcite sample. The peaks

4

116   corresponding to sodium chloride where lower in intensity in the 3g sample compared to the

117   10g sample.

118

119   **Thermal Analysis**

120   Thermogravametric analysis was performed on samples of the hydrotalcite before thermal

121   activation (BTA) and after the adsorption of sulfate. There are only a few possible units that

122   could be lost from the sample as it undergoes decomposition; these include water, carbon

123   dioxide, hydroxyl units and oxygen. As evolved mass spectrometry was not carried out it is

124   impossible to conclusively identify any gases evolved, however as the mechanism of the

125   thermal decomposition of hydrotalcite is described in the litrature it is possible to propose a

126   decomposition mechanism based on previous experiments [1, 20, 21, 10, 22-25, 9, 26-28].

127

128   Six mass losses were observed during the decomposition of hydrotalcite BTA shown in Fig3.

129   The first two peaks occurred at 39 and 69°C and accounted for mass losses of 3.81 and 7.70%

130   respectively. Due to the relatively low temperatures of these mass losses it is fairly safe to

131   assume they correspond to weakly adsorbed water. The next mass loss at 170°C accounted for

132   4.40% of the mass loss. This peak occurs at a high enough temperature for the loss of interlayer

133   water but not high enough for the removal of the carbonate anions or hydroxyl groups.

134

135   The fourth mass loss was the largest occurring at 310°C accounting for 20.44% of the mass

136   loss. When the DTG curve was examined two overlapping features could be clearly

137   distinguished one occurring at approximately 282°C and a second larger feature at 310°C. Mass

138   losses at this temperature range can usually be attributed to loss of interlayer anions. In this

139   case, carbonate (decarbonation) and the loss of hydroxyl groups (dehydroxylation) are

140   proposed to have been removed at this decomposition step. These processes usually overlap

141   and are usually the largest contributor to the mass loss in LDH structures.

142

143   A small mass loss occurred at 698°C with 7.27% mass loss. The final mass loss at 871°C with a

144   percentage mass loss of 13.52 also appeared to have two overlapping features. The first larger

145   feature occurred at 871°C while a much smaller feature was observed at 939°C. The

146   temperature at which these mass losses occur is too high for dehydroxylation or decarbonation.

147   They can most likely be attributed to decomposition of the metal oxide into a spinel phase

148   resulting in the loss of oxygen. The following mechanism can be proposed for the thermal

149   decomposition of the synthetic hydrotalcite. [1, 10, 22-24]

150

151   The first step in the thermal decomposition involves removal of weakly adsorbed water (up to

152   100°C).

153    $MgAl_2CO_3 (OH)_{16} \cdot xH_2O \rightarrow Mg_6Al_2CO_3(OH)_{16} \cdot 4H_2O + (x-4)H_2O$ (2)

154

155   The next step is elimination of interlayer water (100-200°C).

156    $Mg_6Al_2CO_3(OH)_{16} \cdot 4H_2O \rightarrow Mg_6Al_2CO_3(OH)_{16} + 4H_2O$ (3)

157

158   Dehydroxylation and decarbonation then appear to occur simultaneously (200-400°C). The

159   hydroxyl and carbonate groups are lost as water and carbon dioxide, leaving a magnesium/

160   aluminum oxide mixture.

161    $Mg_6Al_2CO_3(OH)_{16} \rightarrow Mg_6O_8Al_2CO_3 + 8H_2O$ (4)

162    $Mg_6O_8Al_2CO_3 \rightarrow (MgO)_6 Al_2O_3 + CO_2$ (5)

163

164   Decomposition of the mixed metal oxide at temperatures above 400°C into a spinel phase

165   resulting in a loss of oxygen.

166    $2((MgO)_6 Al_2O_3) \rightarrow 4MgAlO_2 + 8MgO + O_2$ (6)

167

168   The TG curve of the 3g of reformed hydrotalcite by treatment in a 1000ppm sulfate solution is

169   shown in Fig 4. Three mass losses where were observed. The first mass loss occurred at

170   approximately125°C accounting for 14.53% mass loss. A broad feature is observed in the DTG

171   curve indicating the mass loss is likely due to loss of adsorbed water and interlayer water. The

172   next mass loss occurred at approximately 352°C and accounted for 28.47% mass loss. The

173   increase in decomposition temperature, compared to BTA, may indicate that sulfate anions

174   have been successfully intercalated. The carbonate only hydrotalcite had a decomposition

175   temperature of only 310°C. It is also possible that the increase in decomposition temperature

176   may result from the reformed hydrotalcite having a different structure to that of the original.

177   Once again the DTG curve showed two peaks overlapping at 316 and 352°C. This mass loss

178   was attributed to loss of interlayer anions (carbonate and sulfate) and dehydroxylation

179   (hydroxide). The final mass loss of 3.13% occurred between 632 and 1000°C. Two small broad

180   peaks where observed in the DTG curve in this region.

181

182   Only four mass loss steps where observed in the TG curve of the 10g sample of reformed

183   hydrotalcite, the results are presented in Fig 5. The first mass loss at 171°C can be attributed to

184   the loss of water. The DTG curve shows a broad feature that can likely be attributed to the loss

185   of adsorbed water while the sharp peak at 171°C is most likely due to the loss of interlayer

186   water. The second and largest mass loss occurred at 319°C accounting for 26.77%. A small

187   peak at 368°C was observed in the DTG curve overlapping with the larger peak at 319°C.

188   Comparison of this DTG curve with the DTG curve of the hydrotalcite BTA suggests that the

189   small peak at 368°C represents the loss of intercalated sulfate anions, while the larger peak at

190   319°C is associated with the loss of intercalated carbonate anions. This mass loss is attributed

191   to loss of interlayer anions (carbonate and sulfate) and loss of hydroxyl groups. The next mass

192   loss at 706°C was the smallest with a percent mass loss of only 2.52%. The final mass loss

193   occurred at 841°C with a percent mass loss of 5.46%. A similar mechanism can be proposed

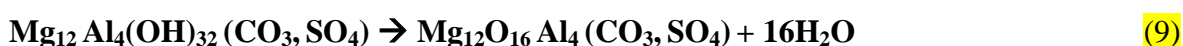194   for the decomposition of the sulfate intercalated LDH.

195

196   Again the first step in the thermal decomposition is the removal of weakly adsorbed water from

197   the surface.

198    $Mg_{12}Al_4(OH)_{32}(CO_3, SO_4) \cdot xH_2O \rightarrow Mg_{12}Al_4(OH)_{32}(CO_3, SO_4) \cdot 8H_2O + (x\text{-}8)H_2O$ (7)

199

200   The next step involves the removal of interlayer water.

201    $Mg_{12}Al_4(OH)_{32}(CO_3, SO_4) \cdot 8H_2O \rightarrow Mg_{12}Al_4(OH)_{32}(CO_3, SO_4) + 8H_2O$ (8)

202

203   The next step involves elimination of the hydroxyl groups as water. Interlayer anions

204   (carbonate and sulfate) will be eliminated in this step most likely as sulfur dioxide and carbon

205   dioxide resulting in the formation of the same mixed metal oxide observed for BTA.

206    $Mg_{12}Al_4(OH)_{32}(CO_3, SO_4) \rightarrow Mg_{12}O_{16}Al_4(CO_3, SO_4) + 16H_2O$ (9)

207    $Mg_{12}O_{16}Al_4(CO_3, SO_4) \rightarrow Mg_{12}O_{16}Al_4O\ CO_3 + SO_2$ (10)

208    $Mg_{12}O_{16}Al_4O\ CO_3 \rightarrow (MgO)_{12}(Al_2O_3)_2 + CO_2$ (11)

209

210   Finally decomposition of the metal oxide can result in the formation of a spinel phase.

211    $(MgO)_{12}(Al_2O_3)_2 \rightarrow 4MgAlO_2 + 8MgO + O_2$ (12)

Conclusions

212
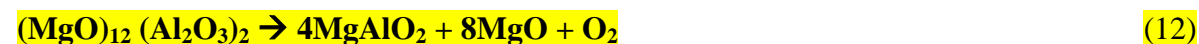
213   Powder XRD indicated the $d_{(003)}$ spacing was within the accepted range for a LDH structure.

214   Thermal activation was found to cause a small increase in the $d_{(003)}$ spacing (0.32 Å).

215   Reformation with sulfate anions caused the $d_{(003)}$ spacing to resemble the $d_{(003)}$ of the original

216   hydrotalcite. It is possible that the majority of sulfate anions are adsorbed on the surface of the

217   regenerated hydrotalcite, while carbonate and a small amount of sulfate has been intercalated

218   into the structure however further investigation is required to confirm this. When the powder

219   XRD patterns were compared to the reference pattern of hydrotalcite a number of characteristic

220   peaks where observed. Several peaks in the powder XRD pattern could be attributed to the

221   presence of sodium chloride. This was not unexpected as it was the main byproduct of the

222   synthesis method used. There results indicate that synthetic Mg/Al hydrotalcite was

223   successfully prepared.

224

225   Comparison of the dehydroxylation and decarbonation temperature indicated that the reformed

226   LDH has intercalated sulfate anions. This is shown by an increase in decomposition

227   temperature of the peak between 300 and 400°C. The carbonate only hydrotalcite had a

228   decomposition temperature of 310°C, while the reformed hydrotalcites from sulfate solutions

229   had a decomposition temperature of 352 and 368°C. All hydrotalcite samples appear to

230   undergo decomposition through a similar mechanism. The similarity of the powder XRD and

231   TG results may indicate that a mixed LDH containing both sulfate and carbonate anions was

232   prepared. The intercalation of carbonate in the reformed hydrotalcites is possible as no attempts

233   where made to prevent the intercalation of carbonate which LDHs have a high affinity for.

234   Further investigation is required to determine the exact composition of the hydrotalcite

235   interlayer.

Acknowledgements

240

241 **References**

242 1. Bouzaid J, Frost RL. Thermal decomposition of stichite. J Therm Anal Calorim.
243 2007;89(1):133-5.

244 2. Frost RL, Erickson KL. Decomposition of the synthetic hydrotalcites mountkeithite and
245 honessite-a high resolution thermogravimetric analysis and infrared emission spectroscopic
246 study. Thermochim Acta. 2004;421(1-2):51-8. doi:10.1016/j.tca.2004.04.008.

247 3. Frost RL, Palmer SJ, Grand L-M. Synthesis and thermal analysis of indium-based
248 hydrotalcites of formula $Mg_6In_2(CO_3)(OH)_{16}.4H_2O$. J Therm Anal Calorim. 2010;101(3):859-
249 63.

250 4. Bakon KH, Palmer SJ, Frost RL. Thermal analysis of synthetic reevesite and cobalt
251 substituted reevesite $(Ni,Co)_6Fe(OH)_{16}(CO_3).4H_2O$. J Therm Anal Calorim. 2010;100(1):125-
252 31.

253 5. Grand L-M, Palmer SJ, Frost RL. Synthesis and thermal stability of hydrotalcites containing
254 gallium. J Therm Anal Calorim. 2009. doi:10.1007/s10973-009-0456-y.

255 6. Grand L-M, Palmer SJ, Frost RL. Synthesis and thermal stability of hydrotalcites containing
256 manganese. J Therm Anal Calorim. 2009. doi:10.1007/s10973-009-0402-z.

257 7. Pesic L, Salipurovic S, Markovic V, Vucelic D, Kagunya W, Jones W. Thermal
258 characteristics of a synthetic hydrotalcite-like material. Journal of Materials Chemistry.
259 1992;2(10):1069-73. doi:10.1039/jm9920201069.

260 8. Rives V. Characterisation of layered double hydroxides and their decomposition products
261 Materials Chemistry and Physics. 2002;75:19-25.

262 9. Frost RL, Palmer SJ, Spratt HJ. Thermal decomposition of hydrotalcites with variable
263 cationic ratios. J Therm Anal Calorim. 2009;95(1):123-9.

264 10. Frost RL, Bouzaid JM, Martens WN. Thermal decomposition of the composite
265 hydrotalcites of iowaite and woodallite. J Therm Anal Calorim. 2007;89(2):511-9.

266 11. Węgrzyn A, Rafalska-Łasocha A, Majda D, Dziembaj R, Papp H. The influence of mixed
267 anionic composition of Mg-Al hydrotalcites on the thermal decomposition mechanism based on
268 in situ study. J Therm Anal Calorim. 2010;99(2):443-57.

269 12. Erickson KL, Bostrom TE, Frost RL. A study of structural memory effects in synthetic
270 hydrotalcites using environmental SEM. Materials Letters. 2004;59(2-3):226-9.
271 doi:10.1016/j.matlet.2004.08.035.

272 13. Grand L-M, Palmer SJ, Frost RL. Synthesis and thermal stability of hydrotalcites based
273 upon gallium. J Therm Anal Calorim. 2010;101(1):195-8. doi:10.1007/s10973-009-0456-y.

274 14. Rives V, Editor. Layered Double Hydroxides: Present and Future. New York: Nova
275 Science Pub Inc 2001.

276   15. Das DP, Das J, Parida K. Physicochemical characterization and adsorption behavior of
277   calcined Zn/Al hydrotalcite-like compound (HTlc) towards removal of fluoride from aqueous
278   solution. Journal of Colloid and Interface Science. 2002;261:213-20.

279   16. Liu R, Frost RL, Martens WN. Absorption of the selenite anion from aqueous solutions by
280   thermally activated layered double hydroxide. Water Research. 2009;43(5):1323-9.
281   doi:10.1016/j.watres.2008.12.030.

282   17. Liang L, Li L. Adsorption behavior of calcined layered double hydroxides towards removal
283   of iodide contaminants. J Radioanal Nucl Chem. 2006;273(1):221-6.

284   18. Palmer SJ, Frost RL. Use of Hydrotalcites for the Removal of Toxic Anions from Aqueous
285   Solutions. Industrial & Engineering Chemistry Research.49(19):8969-76.
286   doi:10.1021/ie101104r.

287   19. Frost RL, Musumeci AW. Nitrate absorption through hydrotalcite reformation. J Colloid
288   Interface Sci. 2006;302(1):203-6. doi:10.1016/j.jcis.2006.06.024.

289   20. Frost R, Bouzaid J, Martens W, Kloprogge T. Thermal decomposition of the syenthetic
290   hydrotalcite woodallite J Therm Anal Calorim. 2006;86(2):437-41.

291   21. Frost RL, Adebajo MO, Erickson KL. Raman spectroscopy of synthetic and natural iowaite.
292   Spectrochimica Acta, Part A: Molecular and Biomolecular Spectroscopy. 2005;61A(4):613-20.
293   doi:10.1016/j.saa.2004.05.015.

294   22. Frost RL, Bouzaid JM, Musumeci AW, Kloprogge JT, Martens WN. Thermal
295   decomposition of the syenthetic hydrotalcite iowaite. J Therm Anal Calorim. 2006 86:437-41.

296   23. Frost RL, Erickson KL. Thermal decomposition of natural iowaite. J Therm Anal Calorim.
297   2004;78(2):367-73.

298   24. Frost RL, Martens WN, Erickson KL. Thermal decomposition of the hydrotalcite. J Therm
299   Anal Calorim. 2005;82:603-8.

300   25. Frost RL, Palmer SJ, Nguyen TM. Thermal decomposition of hydrotalcire with molybdate
301   and vandate anions in the interlayer J Therm Anal Calorim. 2008;92(3):879-86.

302   26. Frost RL, Spratt HJ, Palmer SJ. Thermal decomposition of synthesized layered double
303   hydroxides based upon Mg/(Fe,Cr) and carbonate. Thermochim Acta. 2008(479):1-6.

304   27. Lin Y-H, Adebajo MO, Frost RL, Kloprogge JT. Thermogravimetric analysis of
305   hydrotalcites based on the takovite formula $Ni_xZn_{6-x}Al_2(OH)_{16}(CO_3).4H_2O$. J Therm Anal
306   Calorim. 2005;81:83-9.

307   28. Spratt HJ, Palmer SJ, Frost RL. Thermal decomposition of synthesised layered double
308   hydroxides based upon Mg/(Fe,Cr) and carbonate. Thermochim Acta. 2008;479(1-2):1-6.
309   doi:10.1016/j.tca.2008.08.016.

310

311

312

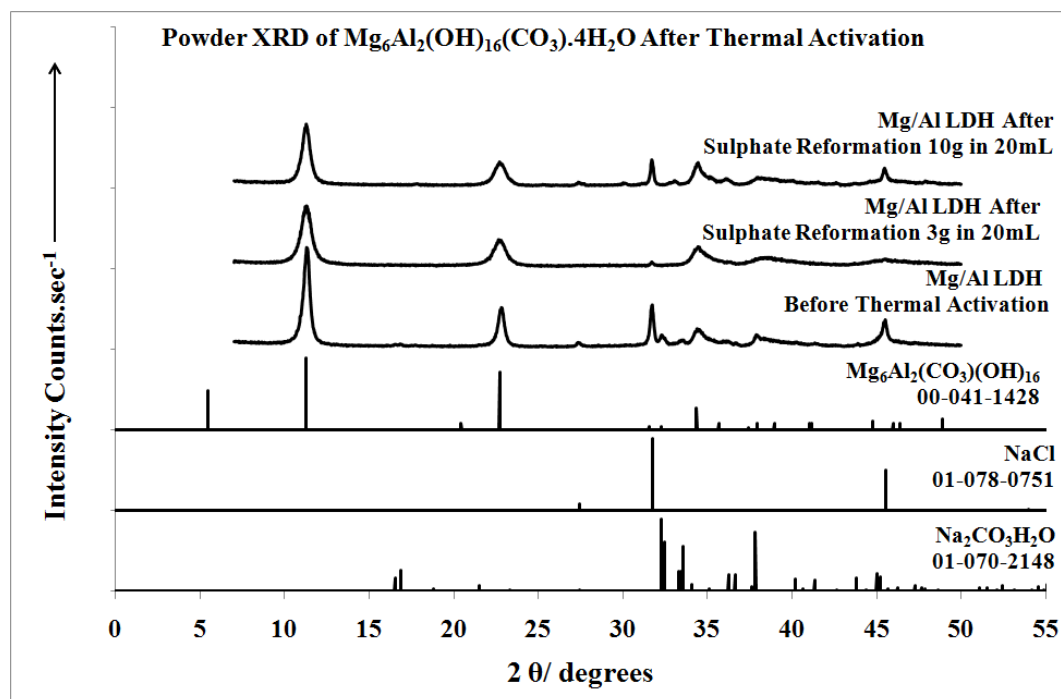313 **Figures**

314

315   Fig 1: XRD pattern of Mg/Al LDH before thermal activation, after treatment of 3 and 10g of Mg/Al LDH in

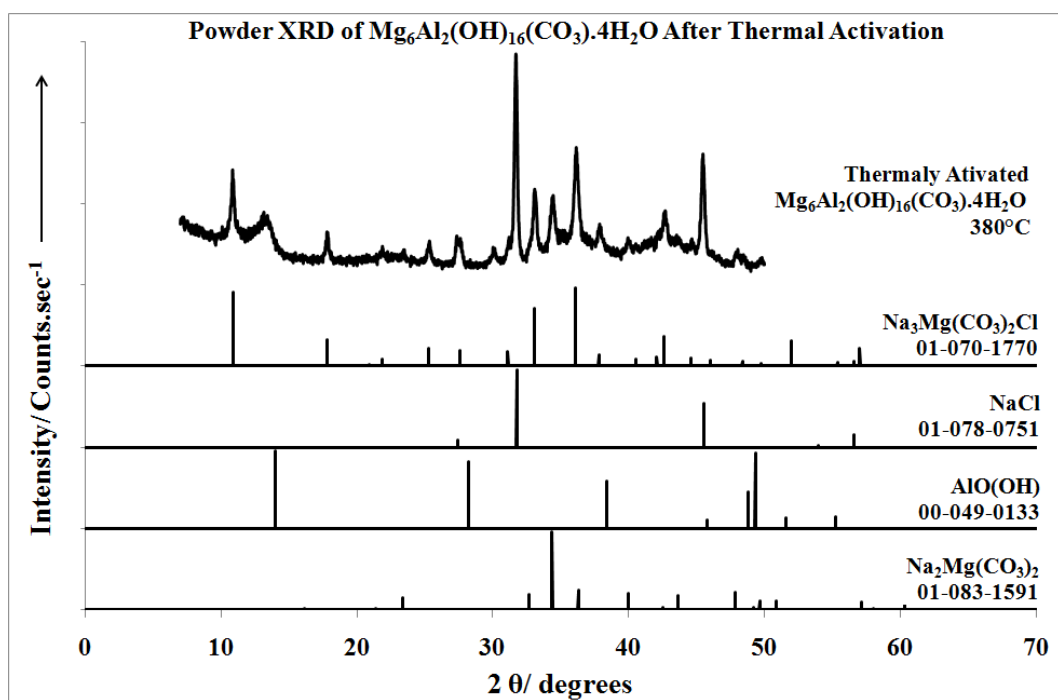316   20cm^3 of sodium sulfate solution and references.

317

318

319

320   Fig 2: XRD pattern of Mg/Al LDH after thermal activation with references of possible phases.
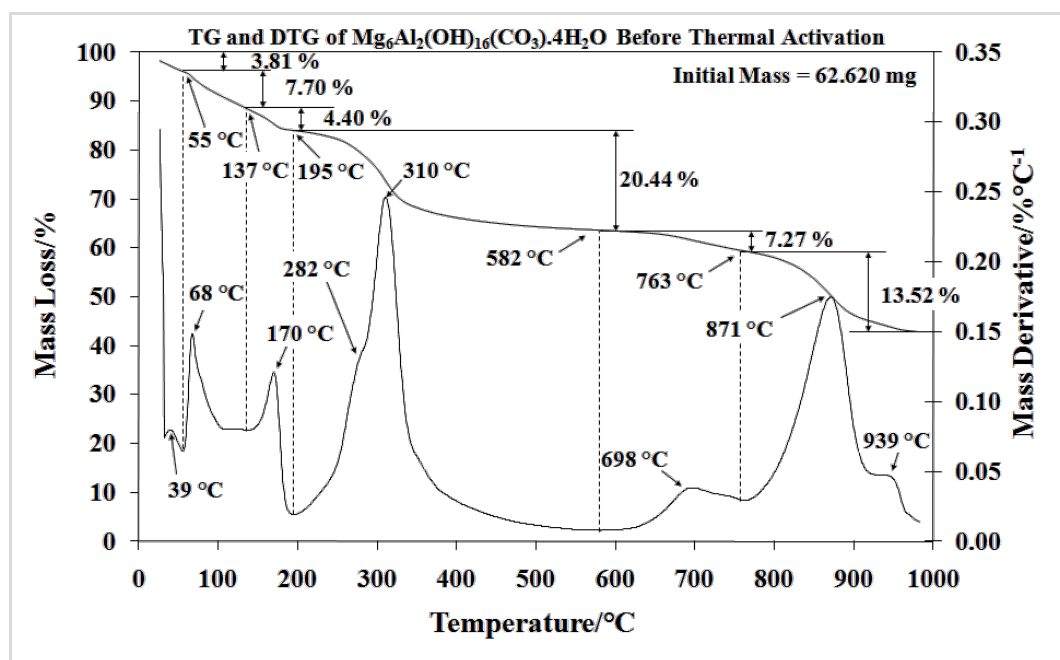
321

322

323

324

325

326

327   Fig 3: TG and DTG curves of Mg/Al LDH Before thermal activation or absorption experiments.
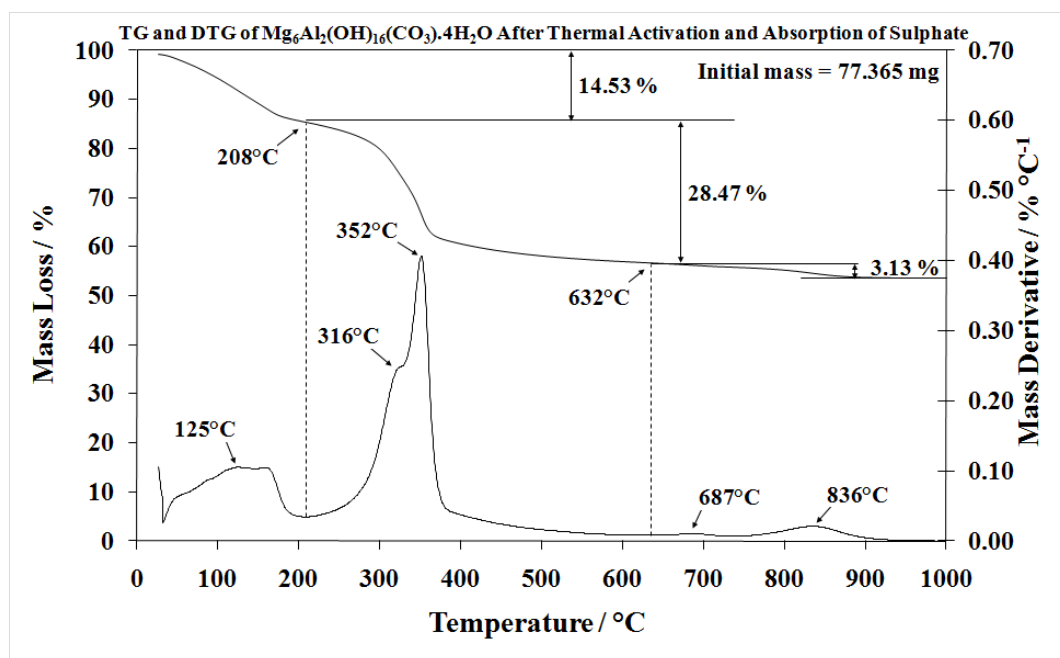
328

329

330

331   Fig 4: TG and DTG curves of Mg/Al LDH After thermal activation and reformation by treatment of 3g of Mg/Al

332   LDH with 1000ppm sodium sulfate solution ($20cm^3$).
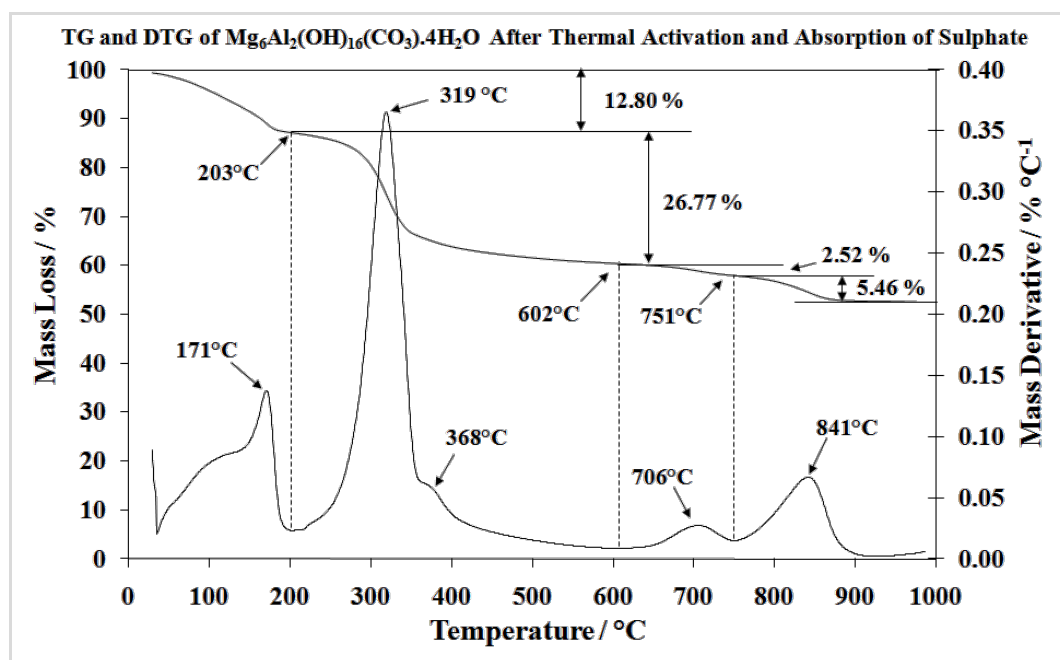
333

334

335

336

337 Fig 5: TG and DTG curves of Mg/Al LDH After thermal activation and reformation by treatment of 10g of Mg/Al

338 LDH with 1000ppm sodium sulfate solution ($20cm^3$).

339

340